Deletion of Mylk1 in Oocytes Causes Delayed Morula-to-Blastocyst Transition and Reduced Fertility Without Affecting Folliculogenesis and Oocyte Maturation in Mice 1

Authors: Liang, Qiu-Xia, Zhang, Qing-Hua, Qi, Shu-Tao, Wang, Zhong-Wei, Hu, Meng-Wen, et al.

Source: Biology of Reproduction, 92(4)

Published By: Society for the Study of Reproduction

URL: https://doi.org/10.1095/biolreprod.114.122127

BIOLOGY OF REPRODUCTION (2015) **92**(4):97, 1–9
Published online before print 11 March 2015.
DOI 10.1095/biolreprod.114.122127

Deletion of *Mylk1* in Oocytes Causes Delayed Morula-to-Blastocyst Transition and Reduced Fertility Without Affecting Folliculogenesis and Oocyte Maturation in Mice[1]

Qiu-Xia Liang,[4,5,6] Qing-Hua Zhang,[4,5] Shu-Tao Qi,[5] Zhong-Wei Wang,[5] Meng-Wen Hu,[4,5] Xue-Shan Ma,[5] Min-Sheng Zhu,[7] Heide Schatten,[8] Zhen-Bo Wang,[3,5] and Qing-Yuan Sun[2,5]

[5]*State Key Laboratory of Reproductive Biology, Institute of Zoology, Chinese Academy of Sciences, Beijing, China*
[6]*University of Chinese Academy of Sciences, Beijing, China*
[7]*Model Animal Research Center and MOE Key Laboratory of Animal Models of Disease, Nanjing University, Nanjing, China*
[8]*Department of Veterinary Pathobiology, University of Missouri, Columbia, Missouri*

ABSTRACT

The mammalian oocyte undergoes two rounds of asymmetric cell divisions during meiotic maturation and fertilization. Acentric spindle positioning and cortical polarity are two major factors involved in asymmetric cell division, both of which are thought to depend on the dynamic interaction between myosin II and actin filaments. Myosin light chain kinase (MLCK), encoded by the *Mylk1* gene, could directly phosphorylate and activate myosin II. To determine whether MLCK was required for oocyte asymmetric division, we specifically disrupted the *Mylk1* gene in oocytes by *Cre-loxP* conditional knockout system. We found that *Mylk1* mutant female mice showed severe subfertility. Unexpectedly, contrary to previously reported in vitro findings, our data showed that oocyte meiotic maturation including spindle organization, polarity establishment, homologous chromosomes separation, and polar body extrusion were not affected in *Mylk1*$^{fl/fl}$;*GCre*$^{+}$ females. Follicular development, ovulation, and early embryonic development up to compact morula occurred normally in *Mylk1*$^{fl/fl}$;*GCre*$^{+}$ females, but deletion of MLCK caused delayed morula-to-blastocyst transition. More than a third of embryos were at morula stage at 3.5 Days Postcoitum in vivo. The delayed embryos could develop further to early blastocyst stage in vitro on Day 4 when most control embryos reached expanded blastocysts. Our findings provide evidence that MLCK is linked to timely blastocyst formation, though it is dispensable for oocyte meiotic maturation.

meiosis, morula-to-blastocyst transition, mouse oocyte, myosin II, myosin light chain kinase (MLCK)

INTRODUCTION

Mammalian oocyte maturation requires two successive rounds of highly asymmetric cell divisions to produce a functional haploid egg. This meiotic program involves several key events critical for asymmetric division in oocyte maturation, including spindle acentric positioning and the establishment of cortical polarity [1]. In meiosis I, following nuclear envelope breakdown, the spindle is initially assembled around the chromosomes at the center of the oocyte. Then the assembled spindle migrates to the subcortical area and becomes localized to the oocyte surface [2], inducing formation of a thickened F-actin cap surrounded by a myosin II ring above the MI spindle [3]. After first polar body extrusion, the meiosis II spindle becomes organized beneath the cortex and maintains its asymmetric position while awaiting fertilization, and a similar myosin II ring is formed and continuously maintained during MII arrest [4, 5]. After fertilization, the MII spindle rotates to be perpendicular to the cortex to facilitate the second polar body extrusion [6]. Studies suggest that dynamic actin filaments [7, 8], which are nucleated by Formin-2 and Spire1/Spire2 [9] in meiosis I and by the Arp2/3 complex [10] in meiosis II, contribute to the spindle's acentric positioning. A question remains concerning how the actin filaments generate the force to promote spindle relocation. Studies show that myosin II, which is enriched at the spindle poles, could pull the actin filaments and generate a force to drive the spindle migration in oocytes [11]; accordingly, myosin II is a key regulator of asymmetric division in oocytes.

Myosin light chain kinase (MLCK) is a Ca^{2+}/calmodulin-dependent, actin and myosin binding, Ser/Thr protein kinase [12]. In smooth muscle, phosphorylation of the 20-kDa regulatory light chain (RLC) of myosin by MLCK is a well-documented event, contributing to the initiation of contraction [13, 14]; furthermore, MLCK could directly phosphorylate myosin II RLC at Thr18/Ser19 to control its assembly and activity in nonmuscle cells [15–17]. Being a critical activator, MLCK participates in various cytoskeleton-related biological processes in nonmuscle cells, including cell motility, contraction, and shape change [18], but there is a lack of research, especially in vivo, on the roles of MLCK in female meiosis and early embryo development.

The purpose of the present study was to investigate the roles of MLCK in folliculogenesis, oocyte maturation, and early embryonic development by conditional gene knockout technology [19, 20] because conventional deletion of MLCK resulted in embryonic or perinatal lethality [21]. In this study, we found that MLCK mutant female mice showed decreased fertility. To investigate the causes of this subfertility, we

[1]This work was supported by the National Basic Research Program of China (2012CB944404 and 2011CB944501) and National Natural Science Foundation of China (Nos. 31272260 and 31201078).
[2]Correspondence: Qing-Yuan Sun, State Key Laboratory of Reproductive Biology, Institute of Zoology, Chinese Academy of Sciences, #1 Beichen West Rd, Chaoyang, Beijing 100101, China.
E-mail: sunqy@ioz.ac.cn
[3]Correspondence: Zhen-Bo Wang, State Key Laboratory of Reproductive Biology, Institute of Zoology, Chinese Academy of Sciences, #1 Beichen West Rd, Chaoyang, Beijing 100101, China.
E-mail: wangzb@ioz.ac.cn
[4]These authors contributed equally to this work.

Received: 4 June 2014.
First decision: 8 July 2014.
Accepted: 6 March 2015.

eISSN: 1529-7268 http://www.biolreprod.org
ISSN: 0006-3363

explored the folliculogenesis, ovulation, oocyte polarity, polar body extrusion, fertilization, and early embryonic development of *Mylk1*mutant females. The results indicated that *Mylk1* mutant females showed delayed blastocyst development with normal follicular development, oocyte maturation, and fertilization, which might explain the reduced litter size.

MATERIALS AND METHODS

Mice

To obtain $Mylk1^{fl/fl};GCre^{+}$ females, we crossed *Gdf9-Cre* (C57BL6 background) [22] with previously reported $Mylk1^{fl/fl}$ mice [14], and the resulting offspring were intercrossed or mated with $Mylk1^{fl/fl}$ mice to generate $Mylk1^{fl/fl};GCre^{+}$ female mice (C57BL6 and 129 mixed background). Unless otherwise specified, the $Mylk1^{fl/fl}$ female mice were used as the control group. DNA extraction from mouse tails was used to genotype the $Mylk1^{fl}$ and $Mylk1^{\Delta}$ alleles. The primer pair for $Mylk1^{fl}$ allele was 1) 5′-TAGTGCGAGTGT CACTGTTG-3′ and 2) 5′-TGACTGGAAAAGGAGCCA-3′. The primer pair for $Mylk1^{\Delta}$ allele was 3) 5′-TAGTGCGAGTGTCACTGTTG-3′ and 4) 5′-CCCCATGATTTGCCTCTAGT-3′. All the animal operations conformed to the guidelines by the Animal Research Committee principles of the Institute of Zoology, Chinese Academy of Sciences. All the mice were housed in a temperature-controlled room with a 12D:12L cycle.

Antibodies

Antibodies used in our experiments were available from the following companies: rabbit monoclonal anti-MLCK antibody (Abcam); rabbit polyclonal anti-phospho-myosin light chain 2 (pMLC2) (Ser19) antibody (CST); mouse monoclonal anti-β-actin antibody (Santa Cruz); goat polyclonal anti-Oct4 antibody (Santa Cruz); rabbit polyclonal anti-Bub3 antibody (Santa Cruz); rabbit monoclonal anti-α-tubulin antibody (CST); fluorescein isothiocyanate (FITC)-conjugated rabbit anti-goat immunoglobulin G (IgG) and FITC-conjugated goat anti-rabbit IgG (Zhongshan Golden Bridge Biotechnology); and Cy5-conjugated goat anti-rabbit IgG (Jackson ImmunoResearch Laboratory).

Western Blot Analysis

For Western blot analysis, 150 germinal vesicle (GV) oocytes were collected in 2× SDS sample buffer and boiled for 5 min at 100°C. Western blot analysis was performed as described previously [23]. Briefly, the separated protein in SDS PAGE were electrically transferred to a polyvinylidene fluoride membrane, and then the membrane was blocked in 50 mM Tris, 150 mM NaCl, and 0.1% Tween (TBST) containing 5% skimmed milk for 2 h, followed by incubation overnight at 4°C with rabbit monoclonal anti-MLCK antibody (1:1000) and mouse monoclonal anti-β-actin antibody (1:1000). After washing three times in TBST, 10 min each time, the membranes were incubated for 1 h at 37°C with peroxidase-conjugated anti-rabbit IgG (1:1000) and peroxidase conjugated anti-mouse IgG (1:1000), respectively. Finally, the membranes were washed three times in TBST and processed for detection with Bio-Rad ChemiDoc XRS+.

Semiquantitative RT-PCR

Total RNA of oocytes was extracted by RNeasy Micro Kit (Qiagen) and reverse transcribed with cDNA synthesis kit (Invitrogen). *Peptidylprolyl isomerase A* (*Ppia*) was used as the control gene to correct the cDNA level of the samples. The primers used were as follows: 1) *Mylk1*: 5′-GATGAAGTG GAAGTGTCCGA-3′ and 5′-CCAGAACCATGACAATGTTG-3′; and 2) *Ppia*: 5′-CGCGTCTCCTTCGAGCTGTTTG-3′ and 5′-TGTAAAGTCAC CACCCTGGCACAT-3′.

Oocyte and Embryo Collection and In Vitro Culture

In our experiments, 6- to 8-wk-old $Mylk1^{fl/fl};GCre^{+}$, $Mylk1^{fl/fl}$, and wild-type females were used. Forty-eight hours after injection of eCG (10 international units [IU]), mice were used to collect GV oocytes or were then administrated hCG (10 IU) to collect MII eggs. To collect preimplantation embryos, the $Mylk1^{fl/fl};GCre^{+}$ females, $Mylk1^{fl/fl}$ females, or superovulated wild-type females were caged with 8-wk-old C57BL/6J wild-type males. Noontime of the day when a vaginal plug was observed was considered as 0.5 Days Postcoitum (dpc). Zygotes were collected from the ampullar region of the oviduct at 0900 h on the day when the vaginal plug was found. Embryos were cultured in vitro to the morula stage in KSOM medium (Millipore) in a humidified 5% CO_2 incubator at 37°C. Blastocysts were flushed from the uterus at 3.5 dpc and then cultured in vitro to 4.0 dpc in KSOM medium.

Immunofluorescence

Immunofluorescent staining was performed according to previously published methods [24]. Briefly, MI oocytes, MII eggs, morula, and blastocysts were fixed for 30 min at room temperature in 2% formaldehyde supplemented with 100 mM HEPES, 50 mM ethylene glycol tetraacetic acid, 10 mM $MgSO_4$, 0.2% Triton X-100 (pH 7, titrated with KOH). Then they were treated with PBS containing 0.1% Triton X-100 overnight at 4°C and incubated with antibodies (MLCK, 1:50; pMLC2, 1:100; α-tubulin, 1:1000; Oct4, 1:500) in PBS, 0.1% Triton X-100, and 3% bovine serum albumin (BSA) overnight at 4°C. DNA was stained with propidium iodide (PI) or 4′,6-diamidino-2-phenylindole (DAPI) for 10 min. The oocytes or embryos were mounted on glass slides and examined with a laser scanning confocal microscope (Zeiss 780 META) and Perkin Elmer Ultra-VIEW VOX confocal Imaging System, respectively.

Fertility Analysis

Eight-week-old C57BL/6J wild-type males were mated with 6-wk-old *Mylk1* mutant females and control siblings. Two females were caged with one male. A total of six *Mylk1* mutant females and six control females were used in this experiment. During a 6-mo period, the cages were monitored daily, and the number and size of the litters were recorded.

Hematoxylin and Eosin Staining and Quantification of Ovarian Follicles

Ovaries were dissected from 8-wk-old mutant and control mice immediately after euthanasia and fixed in 4% formaldehyde overnight, dehydrated with a graded ethanol series, and embedded in paraffin. Paraffin-embedded ovaries were cut into sections of 8-μm thickness and mounted on glass slides. After adequately drying at 48°C overnight, sections were deparaffinized in xylene, hydrated by a graded alcohol series, and stained with hematoxylin and eosin for histological analyses. Ovarian primordial follicles and activated follicles were counted in all the sections of an ovary. Quantification of ovarian follicles was performed as previously reported [25]. In each section, only follicles that contained oocytes with clearly visible nuclei were counted.

Chromosome Spread

Chromosome spread was performed as described previously [26]. Briefly, the zona pellucida of MII eggs was removed by acid Tyrode solution (Sigma). After washing two to three times in M2 medium (Sigma), the oocytes were transferred to glass slides dipped in a solution of 1% paraformaldehyde in distilled H_2O (pH 9.2) containing 0.15% Triton X-100 and 3 mM dithiothreitol. After the slides were dry, they were blocked with 1% BSA for 1 h at room temperature and incubated in anti-Bub3 antibody overnight at 4°C, washed three times and incubated with FITC-conjugated goat anti-rabbit IgG antibody (1:100) for 2 h at room temperature. DNA was stained with PI for 10 min. A laser scanning confocal microscope (Zeiss 710 META) was used for microscopy and image analysis.

Statistical Analysis

All the experiments were performed at least three times. Data were evaluated by Student *t*-test, and $P < 0.05$ was considered statistically significant.

RESULTS

Oocyte-Specific Deletion of the Mylk1 Gene

To obtain oocyte-specific *Mylk1* mutant mice, we crossed $Mylk1^{fl}$ mice in which exons 23–25 were flanked by two *loxP* sites with transgenic mice expressing *Gdf-9* promotor-driven Cre recombinase (Supplemental Fig. S1,A–C; all Supplemental Data are available online at www.biolreprod.org). In *Gdf-9* Cre mice, Cre was expressed from primordial to later follicular stages. PCR genotyping of the pups of $Mylk1^{fl/fl};GCre^{+}$ females mated with wild-type males indicated that recombination occurred in

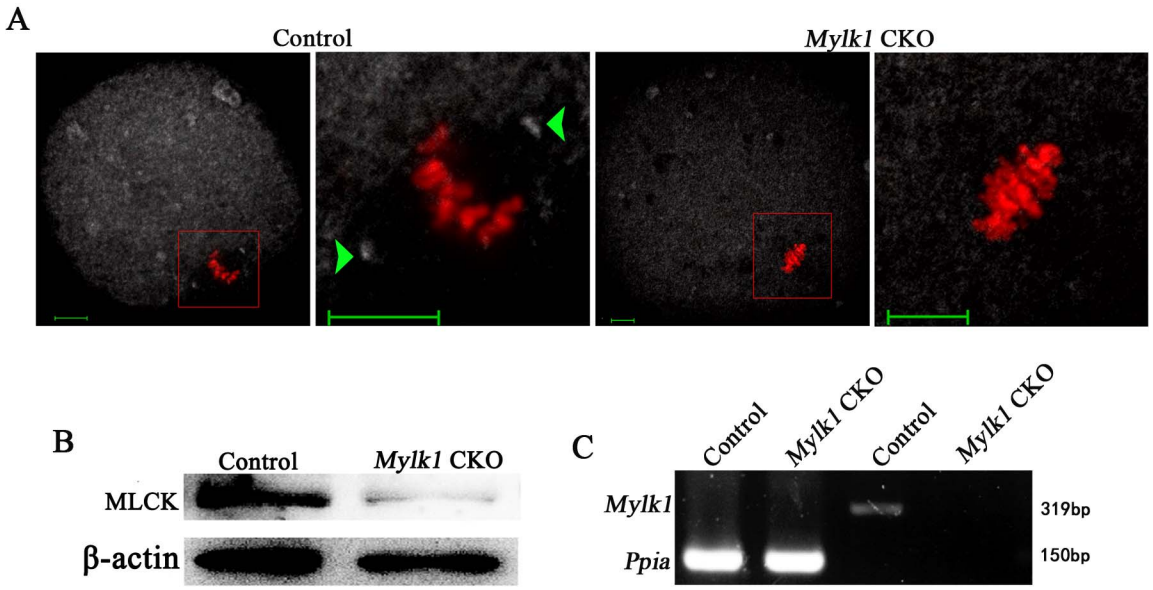

FIG. 1. Verification of loss of *Mylk1* in mouse oocytes. **A**) Immunofluorescence detection of MLCK loss in MII oocytes of *Mylk1*$^{fl/fl}$;*GCre*$^{+}$ mice. The superovulated MII eggs were stained for MLCK (white), and DNA was counterstained with DAPI (red). Boxed regions are magnified in the second images (red box). Colored arrowheads indicate the location of MLCK. Bar = 10 μm. **B**) Western blot detection of MLCK protein levels in oocytes from*Mylk1*$^{fl/fl}$ and *Mylk1*$^{fl/fl}$;*GCre*$^{+}$ mice. **C**) Deletion of *Mylk1* in mutant and control oocytes was determined by semiquantitative RT-PCR. The 319 bp bands correspond to the *Mylk1*, and the 150 bp bands correspond to the *Ppia*.

floxed oocytes (Supplemental Fig. S1D). Immunofluorescent analysis of MII oocytes from *Mylk1*$^{fl/fl}$;*GCre*$^{+}$ mice showed loss of MLCK localization in spindle poles, which indicated the deletion of MLCK protein (Fig. 1A). Immunoblotting and semiquantitative RT-PCR analysis further confirmed that the expression of MLCK in oocytes from *Mylk1*$^{fl/fl}$;*GCre*$^{+}$ mice was efficiently deleted at the mRNA and protein levels (Fig. 1, B and C). However, analysis of MLCK-deleted oocytes showed that pMLC2 (Ser19) localized in one or both spindle poles, which revealed that myosin II was activated in the absence of MLCK (Fig. 2).

Mylk1 *Mutant Females Displayed Subfertility, but Follicular Development Was Not Affected*

To study the effect of oocyte-specific deletion of MLCK on fertility, we conducted a breeding assay. Wild-type males were mated with 6-wk-old *Mylk1* mutant and control females. The results indicated that *Mylk1* mutant females were significantly subfertile (Fig. 3A), generating on average 4.9 offspring per female compared with 10.3 offspring for control females (Fig. 3B). The subfertility could be due to ovarian dysfunction, resulting in functional oocyte loss. However, a comparison of ovarian morphology and the number of primordial and activated follicles in *Mylk1* mutant and control females showed no significant difference. The results indicated that reduced fertility was not caused by follicular abnormality (Fig. 3, C and D).

MLCK Deletion Had No Effect on Meiotic Spindle Organization, Chromosome Alignment, and First Polar Body Extrusion

To determine whether the subfertility was caused by oocyte maturation abnormality, we collected MII eggs from *Mylk1* mutant and control mice after injection of eCG (48 h) and hCG (13 h). The results revealed that *Mylk1* mutant females could ovulate normally, and there was no significant difference in the number of superovulated oocytes from each group (Fig. 4A). Immunofluorescent results showed that the spindle was correctly positioned beneath the cortex and showed normal morphology (Fig. 4B). To evaluate whether the homologous chromosomes were segregated correctly, we performed chromosome spread on superovulated eggs. Centromeric protein Bub3 was stained to assist chromosome counting. Our results indicated that the oocytes had 20 pairs of sister chromatids and they were closely connected at centromeres (Fig. 4C), suggesting that homologous chromosomes were segregated accurately. These findings showed that MLCK-deficient oocytes could undergo normal first meiotic division to produce fully mature eggs.

Fertilization and Embryonic Development up to the Morula Stage Were Not Affected by MLCK Deletion

To analyze if the subfertility was caused by fertilization or early embryonic development failure, we crossed *Mylk1* mutant and control females with wild-type males. The zygotes were collected and cultured in vitro. The results revealed that MLCK-deficient oocytes could be fertilized successfully and form two pronuclei (Fig. 5A). Further culture showed that the zygotes could develop normally to the 2-cell (Fig. 5B) and morula stage (Fig. 5C). These data showed that MLCK-deficient eggs were able to undergo normal second polar body extrusion, fertilization, and development up to the compact morula stage.

MLCK Absence Delayed the Development from the Morula Stage to the Blastocyst Stage

When the 3.5 dpc embryos were flushed from the uterus, we found that an average of 36.6% embryos from *Mylk1* mutant females (n = 5) were in the morula stage compared with only 6.4% morula stage embryos from control females (n = 6). In vitro culture showed that the delayed morula could develop to early blastocyst stage at Day 4, when most control blastocysts

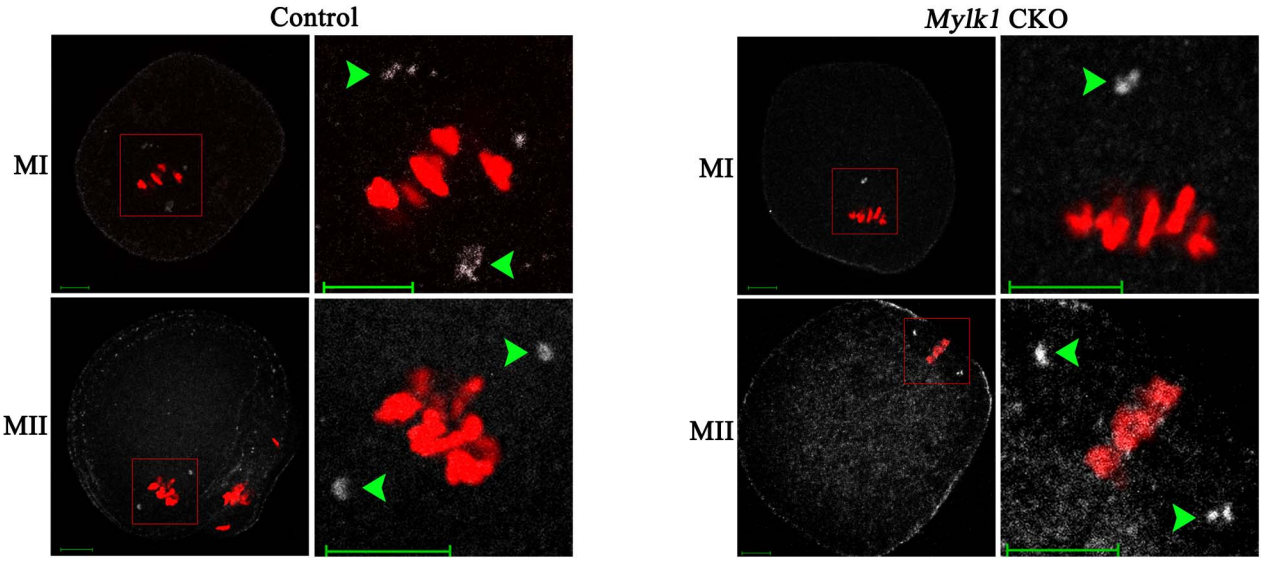

FIG. 2. The presence of pMLC2 (Ser19) at one or two spindle poles at the oocytes of *Mylk1*$^{fl/fl}$ and *Mylk1*$^{fl/fl}$;*GCre*$^{+}$ females, respectively. MI and MII oocytes were collected and stained for pMLC2 (white), and DNA was counterstained with DAPI (red). Boxed regions are magnified in the second images (red box). Colored arrowheads indicate the location of pMLC2. Bar = 10 μm.

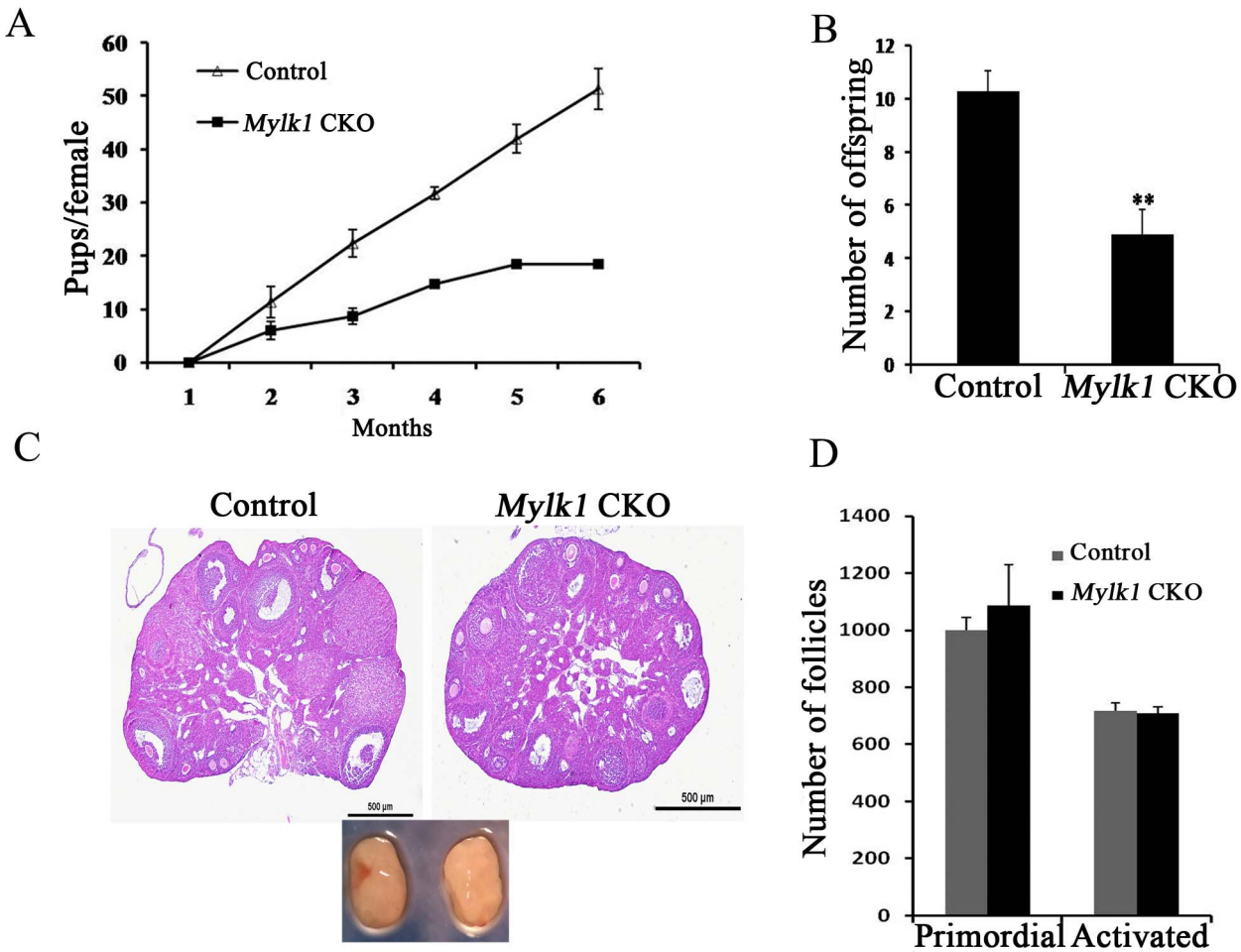

FIG. 3. *Mylk1*$^{fl/fl}$;*GCre*$^{+}$ females displayed subfertility. **A**) Comparison of the accumulative number of pups per *Mylk1*$^{fl/fl}$ female and *Mylk1*$^{fl/fl}$;*GCre*$^{+}$ female. **B**) Comparison of the average number of pups per *Mylk1*$^{fl/fl}$ female and *Mylk1*$^{fl/fl}$;*GCre*$^{+}$ female (n = 6 for both groups). **Significant difference, $P < 0.01$. **C**) Histological images of ovaries of *Mylk1*$^{fl/fl}$ and *Mylk1*$^{fl/fl}$;*GCre*$^{+}$ females. Bar = 500 μm. **D**) Quantification of ovarian follicles in *Mylk1*$^{fl/fl}$ and *Mylk1*$^{fl/fl}$;*GCre*$^{+}$ females. Numbers of primordial and activated follicles per ovary were counted. Error bars denote SEM of three experiments.

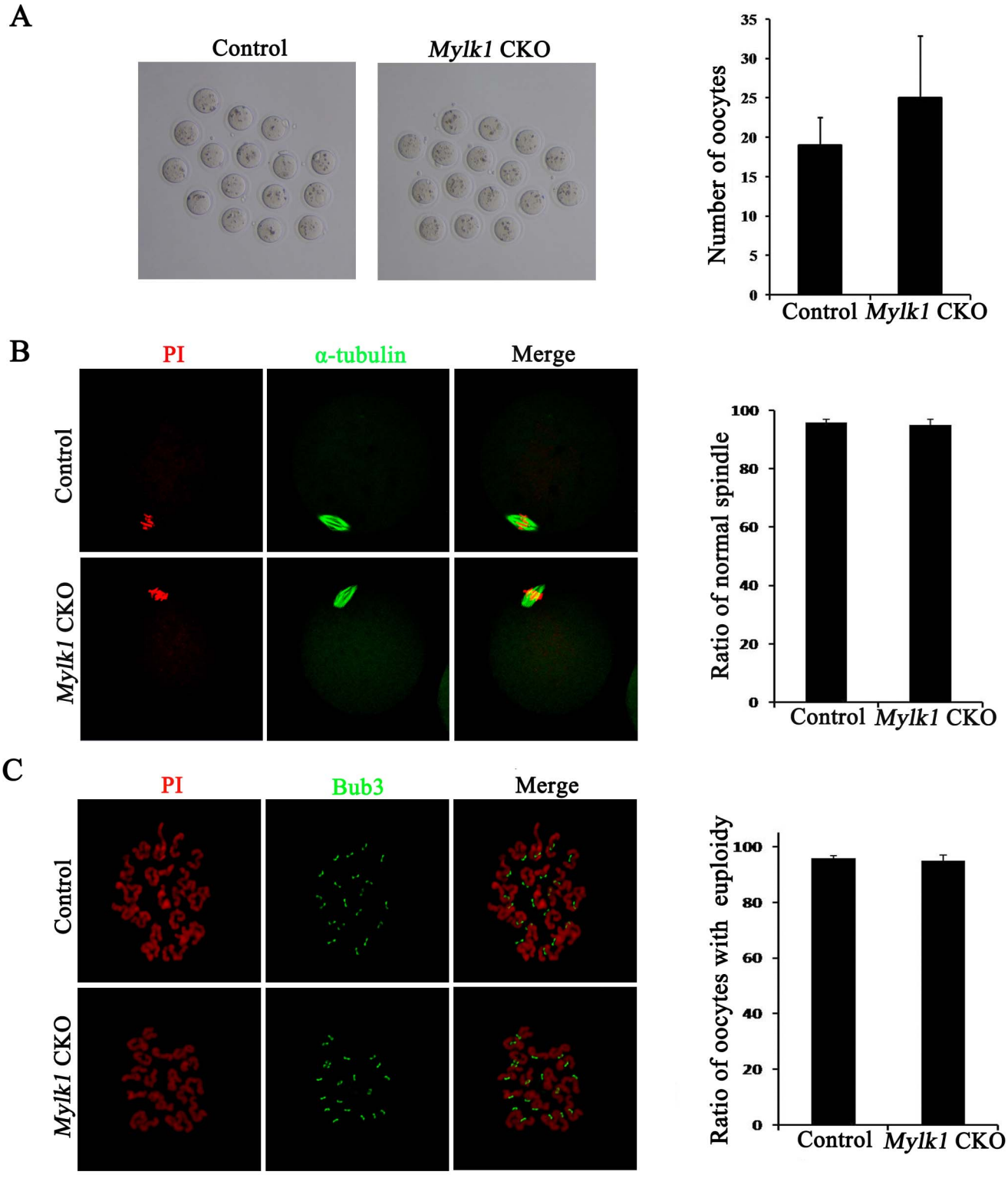

FIG. 4. Evaluation of MII egg quantity and quality of *Mylk1*$^{fl/fl}$ females and *Mylk1*$^{fl/fl}$*;GCre*$^{+}$ females. **A**) Left: microscopic images of MII eggs from mutant and control females. Right: number of MII eggs recovered from *Mylk1*$^{fl/fl}$ females and *Mylk1*$^{fl/fl}$*;GCre*$^{+}$ females. Error bar denotes SEM of five experiments. Original magnification ×20. **B**) Left: confocal microscopic images of spindle morphology and chromosome alignment of control and MLCK-deficient eggs. Eggs were stained with α-tubulin antibody (green) and PI (red) to show spindle morphology and chromosome alignment, respectively. Right: the spindle status was assessed by its shape. Error bars denote SEM of three experiments. Original magnification ×400. **C**) Left: chromosome spread of control and MLCK-deleted eggs. Eggs were stained with Bub3 antibody (green) and PI (red) to assist chromosome counting. Right: ratio of MII eggs with euploidy. Error bars denote SEM of three experiments.

reached expanded blastocysts (Fig. 6A). For the embryos that developed normally to the blastocyst stage, the distribution of cells in trophectoderm and the inner cell mass, total cell number, and Oct4 expression pattern showed no abnormalities (Fig. 6B). Further immunofluorescent staining showed that MLCK was located in the nucleolus of blastomeres at the

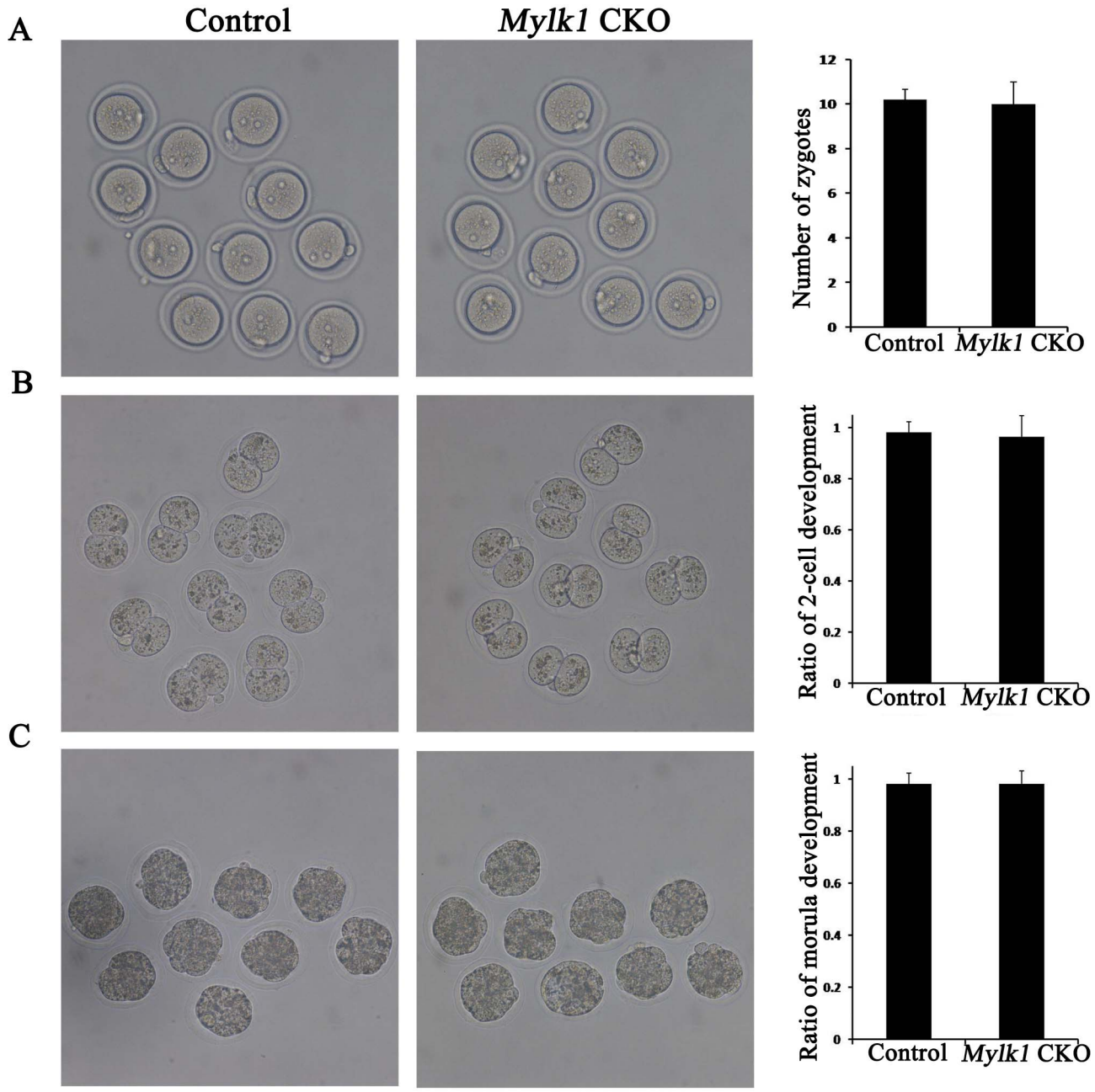

FIG. 5. MLCK-deficient eggs could develop normally to compact morula stages in vitro. **A**) Left: MLCK-deficient eggs could naturally fertilize in vivo. Right: numbers of zygotes. **B**) Left: the fertilized eggs could develop normally to 2-cell stage embryos. Right: average rate of 2-cell development of MLCK-deficient females and wild-type females. **C**) Left: *Mylk1* mutant zygotes could develop normally to compact morula stage. Right: average rate of compact morula development of *Mylk1* mutant and wild-type females. The data are presented as the mean ± SEM of at least three experiments. Original magnification ×20.

morula stage. However, no special signal was found in blastocyst (Fig. 7). These results suggested that MLCK might be involved in timely morula-to-blastocyst transition, which could be the reason for subfertility of *Mylk1* mutant females.

DISCUSSION

In this study, we investigated the roles of MLCK in oocyte meiotic maturation and preimplantation embryonic development by the *Cre-LoxP* system. Compared to the $Mylk1^{fl/fl}$ females, $Mylk1^{fl/fl}$;$GCre^{+}$ females exhibited a sharp reduction in litter size. Quantification of the ovarian follicles in $Mylk1^{fl/fl}$ and $Mylk1^{fl/fl}$;$GCre^{+}$ females indicated that follicular development was not affected in $Mylk1^{fl/fl}$;$GCre^{+}$ females. Analysis of superovulated eggs showed that the MLCK-depleted eggs could form normal spindles and undergo the separation of homologous chromosomes properly. Furthermore, MLCK-deleted oocytes could fertilize and develop normally to the compact morula stage. However, more than a third of the embryos showed delayed blastocyst development. Although these delayed embryos could develop to early blastocysts on Day 4, they may miss the implantation window. Our further experiments showed that MLCK was expressed in nucleolus of blastomeres at compact morula stages, which might be involved in morula-to-blastocyst transition. These findings implied that MLCK might be a maternal-effect gene that was

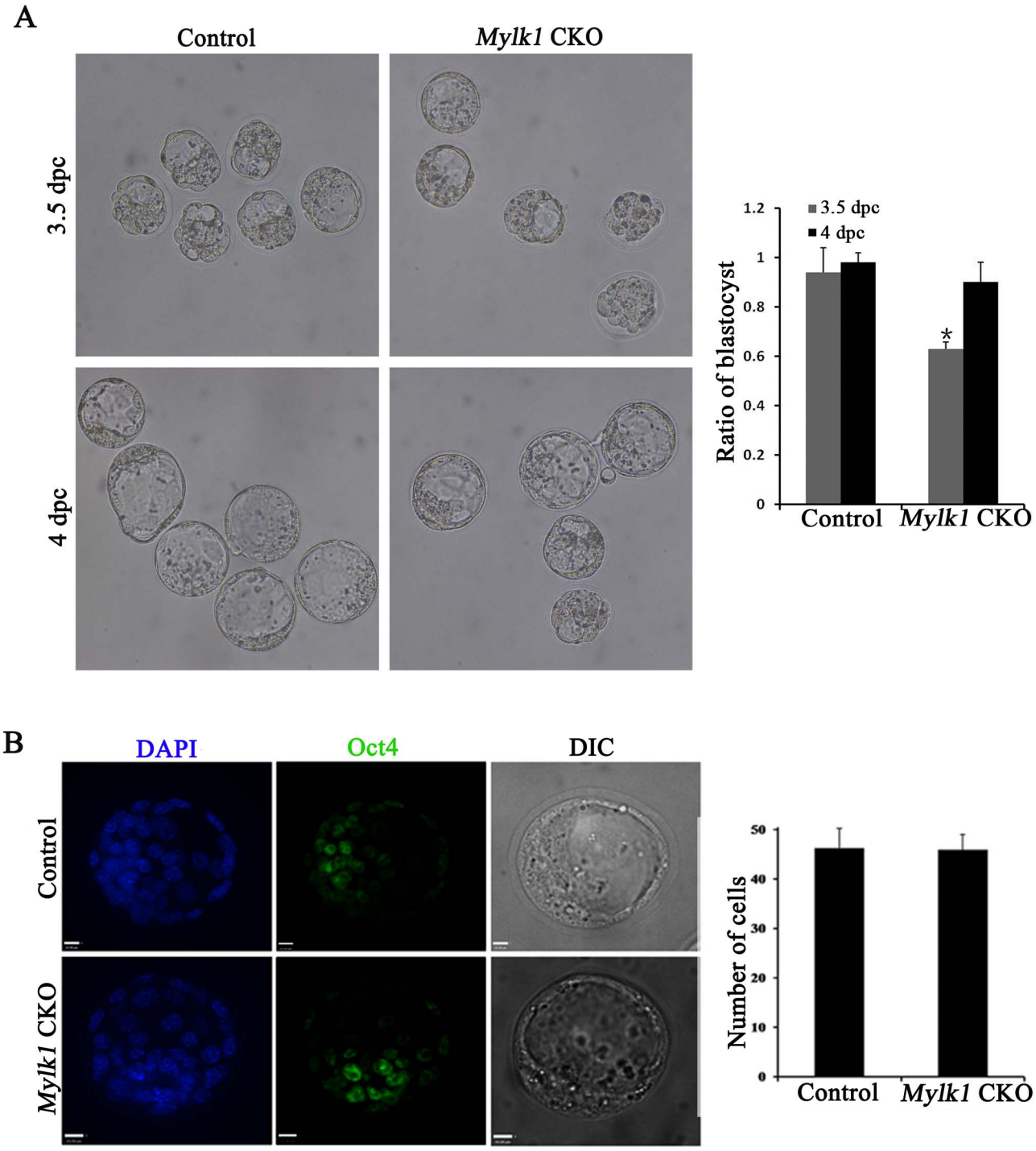

FIG. 6. Delayed morula-to-blastocyst transition of mutant embryos. **A**) Left: microscopic images of 3.5 and 4 dpc embryos from *Mylk1*$^{fl/fl}$ and *Mylk1*$^{fl/fl}$;*GCre* $^{+}$ females. Eight-week-old *Mylk1* mutant and control female siblings were mated with wild-type males. Plugged females were sacrificed at 3.5 dpc. Embryos were collected by uterine flushing and then cultured in vitro to 4 dpc. Right: blastocyst rates were scored based on 3.5 and 4 dpc embryos from *Mylk1*$^{fl/fl}$ and *Mylk1*$^{fl/fl}$;*GCre*$^{+}$ females, respectively. **B**) Left: confocal microscopic images of blastocysts from *Mylk1*$^{fl/fl}$ and *Mylk1*$^{fl/fl}$;*GCre*$^{+}$ females. The collected blastocysts were stained for Oct4 (green). DNA was counterstained with DAPI (blue), and morphology was determined by differential interference contrast (DIC) microscopy.< Right: the average number of total cell in blastocysts from *Mylk1*$^{fl/fl}$ and *Mylk1*$^{fl/fl}$;*GCre*$^{+}$ females, respectively. The data are presented as the mean ± SEM of at least three experiments. Bar = 10 μm.

transcribed during oogenesis and degraded in later embryonic development stages until the activation of the embryonic *Mylk1* gene. We proposed that delayed morula-to-blastocyst transition might be the cause of the subfertility.

Several previous in vitro studies in which inhibitors were used indicated that MLCK might participate in mammalian oocyte maturation by controlling myosin II activity. Specifically, ML-7, an inhibitor of MLCK, can efficiently block polar body extrusion in vitro by slowing down spindle relocation during first meiosis [11, 27, 28]. Furthermore, both blebbistatin, an inhibitor of myosin II, and ML-7 block cortical cap protrusion [28]. In addition, ML-7 inhibits second polar body

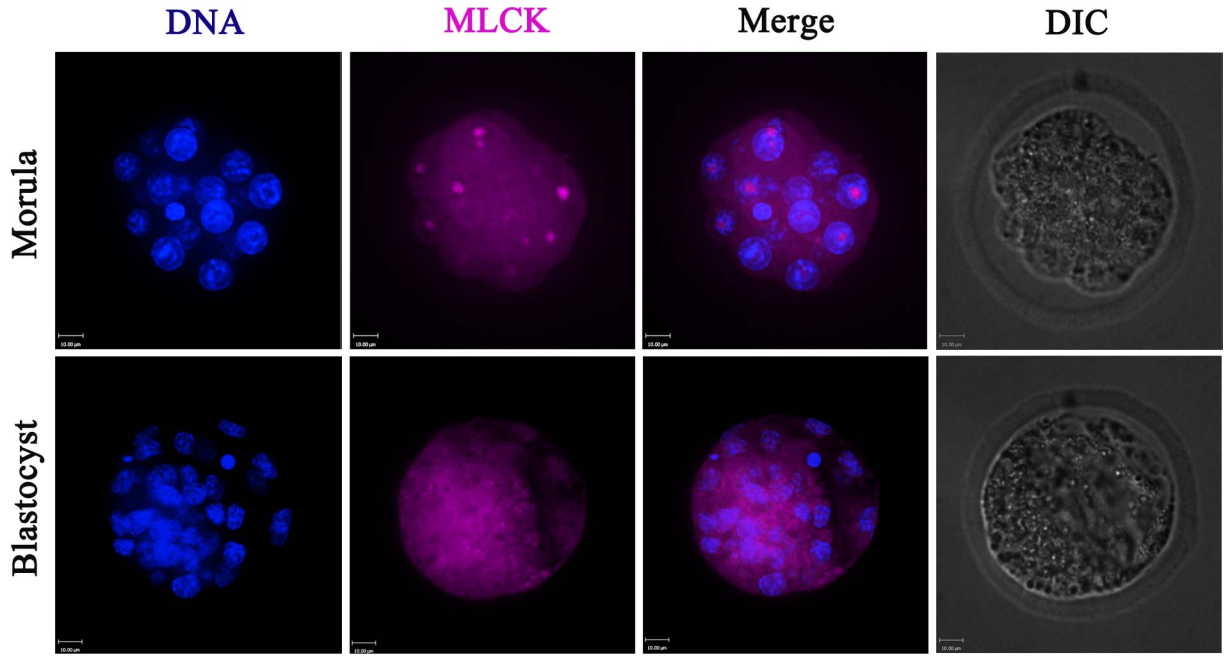

FIG. 7. Immunofluorescence detection of MLCK expression in morula and blastocyst. Morula and blastocysts were collected and stained for MLCK (pink). DNA was counterstained with DAPI (blue), and morphology was determined by differential interference contrast (DIC) microscopy. Bar = 10 μm.

extrusion in a dose-dependent manner, and it reduces cortical granule exocytosis [5, 29]. Another study, however, indicates that neither ML-7 nor blebbistatin can disrupt chromosome movement to the cortex although blebbistatin completely inhibit polar body extrusion [30]. The results of these chemical inhibitor experiments are inconsistent and cannot exclude nonspecific or toxic effects of the inhibitors.

Our in vivo experiment results found that MLCK was located in spindle poles in MII eggs. Strikingly, deletion of MLCK in oocytes caused the loss of its localization, but pMLC2 was still present at the spindle poles. There could be several reasons for this phenotype. One reason is that MLCK deletion might be compensated by other potent myosin II activators. Another reason is that MLCK might not be required for myosin II activation, and the phenotypes displayed in ML-7-treated oocytes might not be caused by MLCK inhibition, but rather by nonspecific inhibition of other proteins or inhibitor toxicity. In summary, oocyte-specific deletion of MLCK does not affect oocyte maturation, fertilization, and early embryo development up to the morula stage, but delays morula-to-blastocyst transition, which may be the reason for reduced fertility.

ACKNOWLEDGMENT

We appreciate Shi-Wen Li, Li-Juan Wang and Hua Qin for their technical assistance. The *Mylk1*$^{fl/fl}$ mice are obtained from the Model Animal Research Center of Nanjing University, Nanjing, China.

REFERENCES

1. Yi KX, Li R. Actin cytoskeleton in cell polarity and asymmetric division during mouse oocyte maturation. Cytoskeleton 2012; 69:727–737.
2. Maro B, Verlhac MH. Polar body formation: new rules for asymmetric divisions. Nat Cell Biol 2002; 4:E281–E283.
3. Deng M, Kishikawa H, Yanagimachi R, Kopf GS, Schultz RM, Williams CJ. Chromatin-mediated cortical granule redistribution is responsible for the formation of the cortical granule-free domain in mouse eggs. Dev Biol 2003; 257:166–176.
4. Simerly C, Nowak G, de Lanerolle P, Schatten G. Differential expression and functions of cortical myosin IIA and IIB isotypes during meiotic maturation, fertilization, and mitosis in mouse oocytes and embryos. Mol Biol Cell 1998; 9:2509–2525.
5. Deng M, Williams CJ, Schultz RM. Role of MAP kinase and myosin light chain kinase in chromosome-induced development of mouse egg polarity. Devel Biol 2005; 278:358–366.
6. Zhu ZY, Chen DY, Li JS, Lian L, Lei L, Han ZM, Sun QY. Rotation of meiotic spindle is controlled by microfilaments in mouse oocytes. Biol Reprod 2003; 68:943–946.
7. Azoury J, Lee KW, Georget V, Rassinier P, Leader B, Verlhac MH. Spindle positioning in mouse oocytes relies on a dynamic meshwork of actin filaments. Cur Biol 2008; 18:1514–1519.
8. Sun QY, Schatten H. Regulation of dynamic events by microfilaments during oocyte maturation and fertilization. Reproduction 2006; 131: 193–205.
9. Montaville P, Jegou A, Pernier J, Compper C, Guichard B, Mogessie B, Schuh M, Romet-Lemonne G, Carlier MF. Spire and Formin 2 synergize and antagonize in regulating actin assembly in meiosis by a ping-pong mechanism. PLoS Biol 2014; 12:e1001795.
10. Liu J, Wang QC, Wang F, Duan X, Dai XX, Wang T, Liu HL, Cui XS, Kim NH, Sun SC. Nucleation promoting factors regulate the expression and localization of Arp2/3 complex during meiosis of mouse oocytes. PLoS One 2012; 7:e52277.
11. Schuh M, Ellenberg J. A new model for asymmetric spindle positioning in mouse oocytes. Curr Biol 2008; 18:1986–1992.
12. Kamm KE, Stull JT. The function of myosin and myosin light chain kinase phosphorylation in smooth-muscle. Annu Rev Pharmacol Toxicol 1985; 25:593–620.
13. Edelman AM, Lin WH, Osterhout DJ, Bennett MK, Kennedy MB, Krebs EG. Phosphorylation of smooth muscle myosin by type II Ca^{2+}/calmodulin-dependent protein kinase. Mol Cell Biochem 1990; 97:87–98.
14. He WQ, Peng YJ, Zhang WC, Lv N, Tang J, Chen C, Zhang CH, Gao S, Chen HQ, Zhi G, Feil R, Kamm KE, et al. Myosin light chain kinase is central to smooth muscle contraction and required for gastrointestinal motility in mice. Gastroenterology 2008; 135:610–620.
15. Adelstein RS, Conti MA. Phosphorylation of platelet myosin increases actin-activated myosin ATPase activity. Nature 1975; 256:597–598.
16. Scholey JM, Taylor KA, Kendrick-Jones J. Regulation of non-muscle myosin assembly by calmodulin-dependent light chain kinase. Nature 1980; 287:233–235.
17. Beach JR, Licate LS, Crish JF, Egelhoff TT. Analysis of the role of Ser1/Ser2/Thr9 phosphorylation on myosin II assembly and function in live cells. BMC Cell Biol 2011; 12:52.
18. Kamm KE, Stull JT. Dedicated myosin light chain kinases with diverse cellular functions. J Biol Chem 2001; 276:4527–4530.
19. Hu MW, Wang ZB, Schatten H, Sun QY. New understandings on

folliculogenesis/oogenesis regulation in mouse as revealed by conditional knockout. J Genet Genomics 2012; 39:61–68.
20. Sun QY, Liu K, Kikuchi K. Oocyte-specific knockout: a novel in vivo approach for studying gene functions during folliculogenesis, oocyte maturation, fertilization, and embryogenesis. Biol Reprod 2008; 79: 1014–1020.
21. Somlyo AV, Wang H, Choudhury N, Khromov AS, Majesky M, Owens GK, Somlyo AP. Myosin light chain kinase knockout. J Muscle Res Cell Motil 2004; 25:241–242.
22. Lan ZJ, Xu XP, Cooney AJ. Differential oocyte-specific expression of Cre recombinase activity in GDF-9-iCre, Zp3cre, and Msx2Cre transgenic mice. Biol Reprod 2004; 71:1469–1474.
23. Qi ST, Wang ZB, Ouyang YC, Zhang QH, Hu MW, Huang X, Ge Z, Guo L, Wang YP, Hou Y, Schatten H, Sun QY. Overexpression of SETbeta, a protein localizing to centromeres, causes precocious separation of chromatids during the first meiosis of mouse oocytes. J Cell Sci 2013; 126:1595–1603.
24. Strickland L, von Dassow G, Ellenberg J, Foe V, Lenart P, Burgess D. Light microscopy of echinoderm embryos. Methods Cell Biol 2004; 74: 371–409.
25. Johnson J, Canning J, Kaneko T, Pru JK, Tilly JL. Germline stem cells and follicular renewal in the postnatal mammalian ovary. Nature 2004; 428: 145–150.
26. Hodges CA, Hunt PA. Simultaneous analysis of chromosomes and chromosome-associated proteins in mammalian oocytes and embryos. Chromosoma 2002; 111:165–169.
27. Larson SM, Lee HJ, Hung PH, Matthews LM, Robinson DN, Evans JP. Cortical mechanics and meiosis II completion in mammalian oocytes are mediated by myosin-II and Ezrin-Radixin-Moesin (ERM) proteins. Mol Biol Cell 2010; 21:3182–3192.
28. Wang Q, Racowsky C, Deng M. Mechanism of the chromosome-induced polar body extrusion in mouse eggs. Cell Div 2011; 6:17.
29. Matson S, Markoulaki S, Ducibella T. Antagonists of myosin light chain kinase and of myosin II inhibit specific events of egg activation in fertilized mouse eggs. Biol Reprod 2006; 74:169–176.
30. Li HB, Guo FL, Rubinstein B, Li R. Actin-driven chromosomal motility leads to symmetry breaking in mammalian meiotic oocytes. Nat Cell Biol 2008; 10:1301–U1101.